

# Simulation of Figure-of-Eight Reentry During Acute Inhomogeneous Myocardial Ischemia: Role of ATP-Sensitive Potassium Current

JM Ferrero (Jr), B Trenor, J Saiz, B Rodriguez

Universidad Politecnica de Valencia, Valencia, Spain

## Abstract

*Figure-of-eight reentry is an abnormal pattern of excitation which is commonly found in hearts subject to acute myocardial regional ischemia. This type of reentry can lead to ventricular tachycardia and fibrillation, which are potentially mortal arrhythmias. In this work, the authors use a detailed mathematical model of the electrical activity of an acutely ischemic tissue to simulate and study this type of reentry. Regional ischemia is modeled by considering the effects of hyperkalemia, hypoxia ( $K_{ATP}$  channel activation) and acidosis in a 2D tissue comprising normal, ischemic and border zone cells. The vulnerable window for reentry was measured for different degrees of  $K_{ATP}$  channel activation. The model successfully simulates figure-of-eight reentry, and the results show that the duration of the vulnerable window depends on the severity of hypoxia in a biphasic manner.*

## 1. Introduction

Ventricular tachycardia and ventricular fibrillation are two well-known potentially mortal arrhythmias which are due to reentrant electrical activity in the ventricles [1]. Although under certain circumstances they may occur in healthy myocardium, they are normally a consequence of the electrophysiological changes caused by acute myocardial ischemia [1,2]. Moreover, if ischemia is of regional nature, the inhomogeneities developed in the myocardium seriously predispose it to reentry [1-5].

A few minutes after coronary artery occlusion, several mapping experiments show that reentrant activity following premature stimulation may have the form of a figure-of-eight, with two parallel reentrant circuits surrounding an area of functional block [3-6]. This pattern may be stable (ventricular tachycardia) or may destabilize, leading to ventricular fibrillation [3,5].

The goal of this work was to theoretically analyse the causes of figure-of-eight reentry during acute regional myocardial ischemia, focusing on the influence of the degree of hypoxia (and, therefore, the degree of activation of the ATP-sensitive  $K^+$  current [7,8]) on the vulnerability to reentry. For this purpose, computer

models were used to simulate electrical activity of a virtual tissue which mimicked the conditions of this type of ischemia. The results show that figure-of-eight reentry likelihood is strongly dependent on the degree of hypoxia in a biphasic manner.

## 2. Methods

In order to simulate the action potentials and underlying ionic currents, we chose the dynamic Luo-Rudy (phase II) equations [9,10] as our basic model due to its comprehensiveness and its electrophysiological detail. To simulate acute ischemia, its three main effects were considered. Firstly, hypoxia was modelled by partially activating the ATP-sensitive  $K^+$  current ( $I_{K(ATP)}$ ), using the formulation of our own group [8]. The degree of  $I_{K(ATP)}$  activation (term  $f_{ATP}$  in the equations in [8], which depends on  $[ATP]_i$  and  $[ADP]_i$ ) was varied through the simulations to study (a) the effects of different degrees of hypoxia, and (b) pharmacological interventions which modulate  $I_{K(ATP)}$ . Secondly, hyperkalemia was simulated by elevating  $[K^+]_o$ . Finally, acidosis was modelled by its effect on the inward  $Na^+$  and  $Ca^{2+}$  currents [11,12].

Although the myocardium is in reality a three dimensional structure, we used a 55x55 mm 2D tissue in our simulations. Figure 1 depicts the structure of the virtual tissue which, in order to properly simulate regional acute ischemia, comprises three distinct zones. A circular shaped central ischemic zone (CZ, 20 mm in diameter [13]) is formed by cells directly affected by the lack of flow. In this zone, the values of the parameters affected by ischemia were chosen to correspond to their experimentally measured values 10 minutes after the onset of ischemia. Specifically, extracellular potassium concentration was set to  $[K^+]_o = 12.5$  mmol/L [7,13] to simulate hyperkalemia; the fast inward  $Na^+$  current ( $I_{Na}$ ) and the  $Ca^{2+}$  current through the L-type channels ( $I_{Ca(L)}$ ) were multiplied by factors  $p_{Na} = p_{Ca} = 0.75$  [11,12], which simulates the main effect of intracellular and extracellular acidosis; and intracellular ATP and ADP concentrations ( $[ATP]_i$  and  $[ADP]_i$ ) were set to 4.6 mmol/L and 100  $\mu$ mol/L respectively [7] (unless otherwise noted) to simulate hypoxia. These values of intracellular ATP and ADP levels yield a fraction of

activated  $K_{ATP}$  channels of 0.7% [8], and are changed through the simulations in order to investigate the effect of different degrees of activation.

In order to represent the actual structure of a regional acute ischemic tissue [1,3,13], a ring-shaped ischemic border zone (BZ) surrounding the CZ was defined in the virtual tissue. According to experimental data from Coronel [13], and choosing a linear approximation for the gradients of the relevant parameters,  $[K^+]_o$  was set to change from 5.4 mmol/L to its ischemic value across the 10 mm BZ. Similarly, the multiplicative factors  $p_{Na}$  and  $p_{Ca}$  were varied from 1.0 to 0.75 across the pH border zone 5 mm in width [11-13]. As for  $[ATP]_i$  and  $[ADP]_i$  (and thus  $f_{ATP}$ ), they were varied across the 1 mm  $pO_2$  border zone [13]. All the mentioned spatial gradients of parameters are graphically shown in Fig. 1.

The simulated tissue was considered anisotropic, and the longitudinal and transverse passive resistances were chosen to yield a longitudinal conduction velocity of approximately 50 cm/s in normal tissue with an anisotropy velocity ratio of 4:1 [14].

The lower side of the tissue was first stimulated with a rectangular pulse 2 ms in duration and 1.5 times diastolic threshold (stimulus  $S_1$ ). A second pulse ( $S_2$ ), simulating a premature stimulus, was applied at the same location with different coupling intervals (CI). The vulnerable window (VW) for reentry was defined as the interval of CIs which yielded reentrant activity in the tissue.

### 3. Results and discussion

In the first set of simulations, we looked for the VW for reentry using the values of the relevant parameters indicated in Fig. 1. In Figs. 2 and 3, the electrical state of the tissue at different time instants is shown. Results are presented as gray-coded voltage snapshots at selected time instants after stimulation.

Figure 2 shows 25 ms-spaced voltage snapshots after the delivery of the first stimulus ( $S_1$ ). The first snapshot, which was taken 50 ms after stimulation, shows expected features of the propagated wavefront. When crossing the NZ, the wavefront is planar and propagates with a longitudinal conduction velocity of 53.4 cm/s. Conduction is slightly accelerated in the external side of the BZ (curved convex wavefront), where mild hyperkalemia is responsible for supernormal conduction. Inside the inner BZ and in the CZ, conduction is delayed due to high hyperkalemia (curved concave wavefront) and conduction velocity is reduced to 22.3 cm/s.

As action potential progresses through the tissue, the CZ and the inner BZ begin to repolarize. In the fifth snapshot (150 ms after stimulation), almost all the CZ and most of the BZ have repolarized while the NZ is still depolarized, indicating that action potentials in the CZ and inner BZ have short durations compared with the NZ [7,8]. This, in turn, is due to the fact that the degree of activation of  $K_{ATP}$  channels considered in the simulation

reduces action potential duration to 46% of its normal value in the NZ [8].

In the last snapshot of Fig. 2 (225 ms after the delivery of  $S_1$ ), only the distal part of the NZ is yet in the repolarization process. The stimulus has generated a completely propagated action potential, with no conduction block occurring at this stage.

Different simulations were carried out in which a second stimulus ( $S_2$ ) was delivered at different CIs at the same location as  $S_1$ . For values of CI higher than 221 ms, no reentry was observed: either an action potential propagated through the whole tissue, or a bi-directional block occurred. For CI values lower than 208 ms, a bidirectional clock in the proximal side of the BZ was found. However, in the window of CIs [208-221], a pattern of figure-of-eight reentry was developed which resembled those obtained experimentally [3-6]. Figure 3(a) shows 12 voltage snapshots of the tissue separated by 50 ms after it has been stimulated by the second stimulus with a CI of 218 ms. In the first and second snapshots (50 and 100 ms after the delivery of  $S_2$ , respectively), a conduction block can be identified in the proximal part of the BZ. In the second and third snapshots, the wavefront is seen to be surrounding the zone of block, which is still in its refractory period (not shown). In the fourth and fifth snapshots, the wavefront is retrogradely invading the CZ, once its refractory period has finished and it has recovered excitability. In the sixth and seventh snapshot, the propagated action potential is re-emerging in the proximal side of the NZ and reentry is being developed. From the eighth to the tenth snapshot, an ectopic beat is being produced, with the wavefront re-exciting zones which had been previously excited by  $S_2$ . Finally, a conduction block can be observed in the distal part of the BZ, and finally the whole tissue returns to rest (twelfth snapshot).

Thus, the VW for reentry, given the ischemic conditions depicted in Fig. 1, had a duration of 13 ms. Inside this window, the premature stimulus  $S_2$  induced one single complete reentrant circuit. The pattern of excitation showed in Fig. 3(a) is very similar to those obtained experimentally under regional acutely ischemic conditions (e.g. see Fig. 8 in [3], Fig. 3 in [4] or Fig. 5 in [6]). The mechanisms that cause the unidirectional block in the proximal part of the BZ are similar in our simulations than in the experiments: the development of postrepolarization refractoriness in the zones with severe hyperkalemia (CZ and inner part of the BZ) makes this part of the tissue unexcitable when the incoming wavefront arrives, and the low conduction velocity with which the wavefront surrounds the zone of block gives time to this zone to recover excitability.

In order to study the effect of the degree of  $K_{ATP}$  channel activation on the likelihood of reentry, and looking for situations which could lead to self-sustained reentry (and not only a single reentrant circuit), we

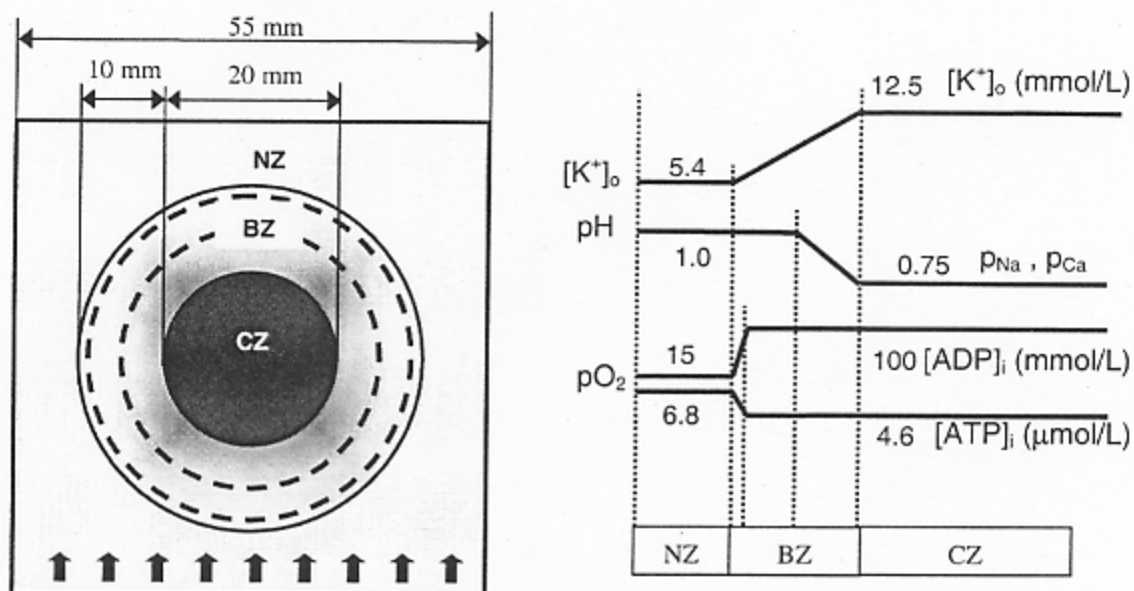


Figure 1. Schematic of the 2D virtual tissue. Left panel: structure of the tissue. Right panel: variations of relevant parameters affected by ischemia (see text for details).

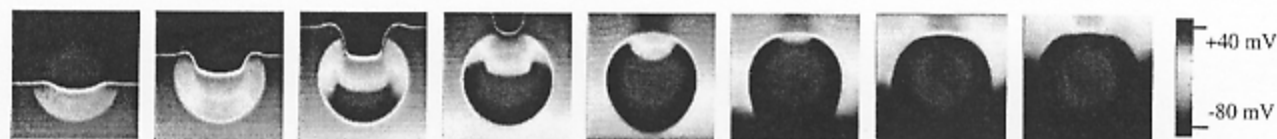


Figure 2. Grey-coded voltage snapshots of the virtual tissue after stimulation with  $S_1$ . Snapshots are separated by 25 ms intervals.

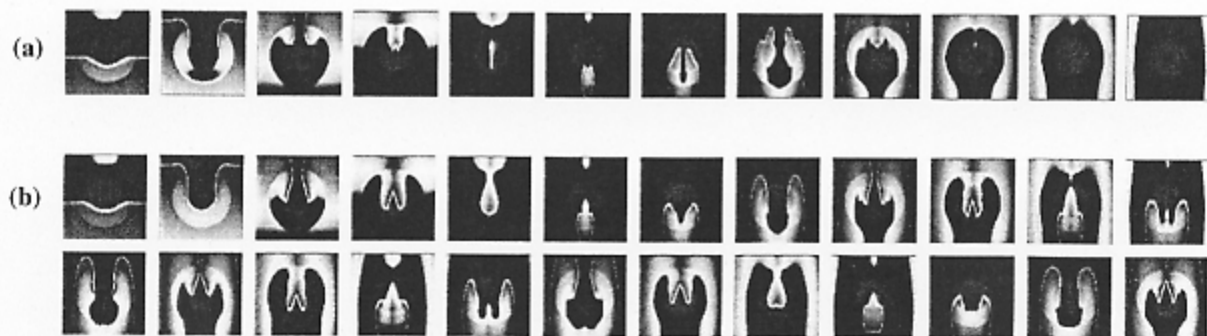


Figure 3. Grey-coded voltage snapshots of the virtual tissue after stimulation with  $S_2$ . Snapshots are separated by 50 ms intervals. (a) Reentry with severe hypoxia. (b) Reentry with mild hypoxia (see text for details)

repeated the simulations for different values of  $[ATP]_i$  and  $[ADP]_i$ , which yielded different figures for  $f_{ATP}$ . Figure 3(b) shows different voltage snapshots corresponding to  $f_{ATP} = 0.39\%$  (mild activation of  $K_{ATP}$  channels). The figure shows that a different pattern of figure-of-eight reentry is obtained, and that more than one reentrant circuit appears. Conversely to the case of Fig. 3(a), no conduction block is developed when the first reentrant waveform reaches the distal part of the BZ (snapshots ninth and tenth), and four complete ectopic beats can be seen in the figure. When the simulation finished (2000 ms after the delivery of  $S_2$ ), reentrant activity was still present with no other stimuli being applied.

The duration of the VW was measured for different degrees of activation of  $K_{ATP}$  channels ( $f_{ATP}$ ). The likelihood of reentry depended on  $f_{ATP}$  in a biphasic manner. For  $f_{ATP} = 0.07\%$  ( $K_{ATP}$  channels practically closed), premature stimulus could not induce reentry regardless of the CI (VW duration = 0). The same situation occurred for  $f_{ATP} \geq 1.0\%$ . For intermediate values of  $f_{ATP}$ , reentry was obtained, with the VW peaking at 45 ms for  $f_{ATP} = 0.39\%$ , which correspond to mild activation of  $K_{ATP}$  channels. For  $f_{ATP} = 0.25\%$ , the VW duration was 32 ms, and  $f_{ATP} = 0.7\%$  yielded a VW duration of 13 ms.

#### 4. Conclusions

Figure-of-eight reentry, an arrhythmic phenomenon obtained experimentally under conditions of regional acute ischemia, was successfully simulated using a comprehensive action potential and ionic current model, together with a model of ischemia in a realistically inhomogeneous anisotropic virtual heart tissue. The patterns of excitation that arose from our simulations closely resembled those obtained under similar experimental conditions. The vulnerable window for reentry peaks at intermediate degrees of  $K_{ATP}$  channel activation. These results encourage the possibility of using pharmacological agents that modulate  $K_{ATP}$  channel activation (e.g. glibenclamide – a  $K_{ATP}$  channel blocker – and pinacidil – a  $K_{ATP}$  channel activator) as antiarrhythmic agents.

#### Acknowledgements

This work was partially supported by the Plan Nacional de Investigación Científica, Desarrollo e Innovación Tecnológica del Ministerio de Ciencia y Tecnología of Spain (TIC 2001-2686).

#### References

- [1] Wit A, Janse J. The ventricular arrhythmias of ischemia and infarction. Electrophysiological mechanisms. Ed Futura Publishing Co 1993.
- [2] Janse MJ, Wit AL. Electrophysiological mechanisms of ventricular arrhythmias resulting from myocardial ischemia and infarction. *Physiol Rev* 1989;69(4):1049-1169.
- [3] Janse MJ, van Capelle FJL, Morsink H, Kleber AG, Wilms-Schopman F, Cardinal R, Naumann C, Durrer D. Flow of "injury current" and patterns of excitation during early ventricular arrhythmias in acute regional myocardial ischemia in isolated porcine and canine hearts. *Circ Res* 1980;47(2):151-165.
- [4] Janse MJ, Kleber AG. Electrophysiological changes and ventricular arrhythmias in the early phase of regional myocardial ischemia. *Circ Res* 1981;49(5):1069-1081.
- [5] Kleber AG. Conduction of the impulse in the ischemic myocardium – implications for malignant ventricular arrhythmias. *Experientia* 1987;43(10):1056-1061.
- [6] Costeas C, Peters NS, Waldecker B, Ciaccio EJ, Wit AL, Coromilas J. Mechanisms causing sustained ventricular tachycardia with multiple QRS morphologies. *Circulation* 1997;96(10):3721-3731.
- [7] Weiss JN, Venkatesh N, Lamp ST. ATP-sensitive  $K^+$  channels and cellular  $K^+$  loss in hypoxic and ischaemic mammalian ventricle. *J Physiol (Lond)* 1992;447:649-673.
- [8] Ferrero JM (Jr), Saiz J, Ferrero JM, Thakor N. Simulation of action potentials from metabolically impaired cardiac myocytes. Role of ATP-sensitive  $K^+$  current. *Circ Res* 1996;79:208-221.
- [9] Luo CH, Rudy Y. A dynamic model of the cardiac ventricular action potential. I. Simulations of ionic currents and concentration changes. *Circ Res* 1994;74:1071-96.
- [10] Zeng J, Laurita KR, Rosenbaum DS, Rudy Y. Two components of the delayed rectifier  $K^+$  current in ventricular myocytes of the guinea pig type. Theoretical formulation and their role in repolarization. *Circ Res* 1995;77(1):140-152.
- [11] Yatani A, Brown AM, Akaike N. Effect of extracellular pH on sodium current in isolated, single rat ventricular cells. *J Membr Biol*, 1984;78(2):163-168.
- [12] Irisawa H, Sato R. Intra- and extracellular actions of proton on the calcium current of isolated guinea pig ventricular cells. *Circ Res* 1986;59(3):348-355.
- [13] Coronel R. Heterogeneity in extracellular potassium concentration during early myocardial ischemia and reperfusion: implications for arrhythmogenesis. *Cardiovasc Res* 1994;28(6):770-777.
- [14] Leon LJ, Roberge FA, Vinet A. Simulation of two-dimensional anisotropic cardiac reentry: effects of the wave length on the reentry characteristics. *Ann Biomed Eng* 1994;22(6):592-609.

Address for correspondence.

José M. Ferrero (Jr)  
 Universidad Politécnica de Valencia  
 Camino de Vera s/n  
 Valencia 46022, Spain.  
 cferrero@eln.upv.es